

EFFECT OF COMBINATIONS OF DIFFERENT OPERATING PARAMETERS ON PERFORMANCE OF PROTON EXCHANGE MEMBRANE FUEL CELL

by

**Prem Kumar THIYAGARAJAN^{a*}, Kanchana JEGANATHAN^b,
Manoj Kumar PANTHALINGAL^a, and Naveen RAJAPPA^a**

^a PSG Institute of Technology and Applied Research, Coimbatore, India

^b PSG College of Technology, Coimbatore, India

Original scientific paper

<https://doi.org/10.2298/TSCI201120070T>

The present study mainly focuses on the different combinations of significant operating parameters like inlet relative humidity of anode gas and cathode gas, operating pressure, and nature of cathode gas on the performance of proton exchange membrane fuel cell using validated 3-D, single-phase, and non-isothermal model with the help of ANSYS FLUENT 18.1 package. The results of different combinations on the performance of proton exchange membrane fuel cell are compared with independent effects of the operating parameters. Results revealed that the combined operating parameters' effect on the performance of the proton exchange membrane fuel cell is deviated significantly (up to 5%) compared to the expected summation of individual parameters effect which is considerable in fuel cell scaling and stack applications. Nature of gas, operating pressure, and inlet cathode gas relative humidity are the most significant parameters in the automobile applications which have to be dealt with care where the combination of changes in operating parameters is quite phenomenal.

Key words: *proton exchange membrane fuel cell, operating parameters, independent effect, combined effect, deviation, ANSYS FLUENT 18.1*

Introduction

Proton exchange membrane fuel cell (PEMFC) is one of the promising technologies for automotive applications because of its low operating temperature (50-80 °C). Optimization of fuel cell operating parameters is one of the key areas of research using simulation and experimental validation. Before the advent of high computing devices, 1-D and 2-D models were preferred by many researchers [1]. Parameters like electro-osmotic drag coefficient, water diffusivity, transport of reactant gases through gas diffusion layers, and electrical conductivity were analyzed in detail. After the availability of high computing devices and commercial modeling packages, the formulation of 3-D models was mostly preferred [2]. Velocity, pressure, and current density contours in different zones, the water content in the membrane, effect of flow channel design on the performance of PEMFC were studied in detail [3-6]. The comparison of flow fields like straight channel and serpentine flow channels were done and their significance on average current density (15000 A/m² and 24500 A/m², respectively) were dis-

* Corresponding author, e-mail: prem50567@gmail.com

cussed [7-9]. The humidity of reactant gas is one of the critical parameters (max at 60% RH) which impact the performance of the PEMFC and it is dependent on different innovative flow designs too [10-13]. The positive effect of porosity and adverse effect of thickness of membrane were also analyzed [14]. The effect of different operating parameters like operating temperature, operating pressure, inlet hydrogen gas temperature, inlet oxygen gas temperature, and cell temperature on the performance of PEMFC was also studied [15-19]. Apart from direct oxygen PEMFC type, the effect of operating and design parameters like operating pressure, orientation, and convection mode of air suction of air-breathing PEMFC on its performance [20-22] were also studied. Researches were extended to fuel cell stack as scaling up of single cell for practical applications and the effect of parameters like the number of cells (inversely proportional to current density), operating parameters on performance were analyzed [23, 24]. The results of different researches on the effect of operating parameters on PEMFC performance are also reviewed and summarized [25-31].

According to the authors' perspective, although a lot of research [15-31] has been done in the area of the effect of operating parameters on performance PEMFC, none of them has concentrated on the combined effect of operating parameters which will be significant in the practical applications. In this research, four different combinations of operating parameters are chosen and their performance deviations are compared with independent effects with the help of simulation results.

Methodology

Governing equations

The conservation of mass, eqs. (1)-(4), momentum, x -direction eq. (5), similarly for y - and z -directions, and energy, eq. (6), are three basic conservation equations which are used to solve along with electro-chemical equations like charge equations, eq. (7) for electron, eq. (8) for proton, and Butler Volmer equations, eq. (9) and (10) [13]:

$$u \frac{\partial(\rho y_i)}{\partial x} + v \frac{\partial(\rho y_i)}{\partial y} + w \frac{\partial(\rho y_i)}{\partial z} = \frac{\partial(j_{x,i})}{\partial x} + \frac{\partial(j_{y,i})}{\partial y} + \frac{\partial(j_{z,i})}{\partial z} + S_i \quad (1)$$

$$S_{H_2} = -\frac{M_{H_2}}{2F} R_{an} \quad (2)$$

$$S_{O_2} = -\frac{M_{O_2}}{2F} R_{cat} \quad (3)$$

$$S_{H_2O} = -\frac{M_{H_2O}}{2F} R_{cat} \quad (4)$$

$$u \frac{\partial(\rho u)}{\partial x} + v \frac{\partial(\rho u)}{\partial y} + w \frac{\partial(\rho u)}{\partial z} = -\frac{\partial p}{\partial x} + \frac{\partial}{\partial x} \left\{ \mu \frac{\partial u}{\partial x} \right\} + \frac{\partial}{\partial y} \left\{ \mu \frac{\partial u}{\partial y} \right\} + \frac{\partial}{\partial z} \left\{ \mu \frac{\partial u}{\partial z} \right\} - \frac{\mu u}{\beta_x} \quad (5)$$

$$\nabla(k\nabla T) = -R_{ohm} I^2 \quad (6)$$

$$\nabla(\sigma_{sol} \nabla \phi_{sol}) + R_{sol} = 0 \quad (7)$$

$$\nabla(\sigma_{\text{mem}} \nabla \varphi_{\text{mem}}) + R_{\text{mem}} = 0 \quad (8)$$

$$R_{\text{an}} = R_{\text{an}}^{\text{ref}} \frac{C_{\text{H}_2} \gamma^{\text{an}}}{C_{\text{H}_2}^{\text{ref}}} \left(e^{\frac{\alpha_{\text{an}} F}{RT} \eta_{\text{an}}} - e^{-\frac{\alpha_{\text{cat}} F}{RT} \eta_{\text{cat}}} \right) \quad (9)$$

$$R_{\text{cat}} = R_{\text{cat}}^{\text{ref}} \frac{C_{\text{O}_2} \gamma^{\text{cat}}}{C_{\text{O}_2}^{\text{ref}}} \left(e^{-\frac{\alpha_{\text{cat}} F}{RT} \eta_{\text{cat}}} - e^{\frac{\alpha_{\text{an}} F}{RT} \eta_{\text{an}}} \right) \quad (10)$$

where u , v , and w [ms^{-1}] are velocity at x -, y -, and z -directions respectively, ρ [kgm^{-3}] – the density of fluid, y_i and $j_{x,i}$, $j_{y,i}$, $j_{z,i}$ – the mass fractions and diffusion mass flux vectors in x -, y -, and z -directions, respectively, S_i [$\text{kgs}^{-1}\text{m}^{-3}$] – the mass sink terms and can be found out separately for H_2 , O_2 , and H_2O separately using equations eqs. (2)-(4), M [kgmol^{-1}] – the molecular weight of different species, and F [Cmol^{-1}] – the Faraday's constant, R_{an} and R_{cat} [Am^{-3}] – the exchange current densities at anode and cathode, respectively, which can be found out using eq. (9) and (10).

Assumptions and boundary conditions

A 3-D model of a single flow channel is considered along with non-isothermal assumptions. The laminar model is chosen based on the Reynolds number. It is assumed that the water vapor formed during the oxidation process is not condensed and leaves the fuel cell as vapor itself (single-phase model). It is also assumed that the reactant gas behaves like an ideal gas. The gas diffusions layer is assumed to be homogeneous and isotropic in nature. No-slip boundary condition was also given for boundary walls. Grid independence was analysed and optimum mesh size was chosen. The boundary conditions for model validation are given in tab. 1. The same boundary conditions are used in operating parameters analysis but with the variation in numerical values for different combinations analysis.

Numerical procedure and model validation

The geometry of the single-channel in three dimensions was drafted using inbuilt DESIGN MODELER software as shown in fig. 1 and meshing is done using structured meshes. The boundary conditions were solved by the SIMPLE algorithm and implicit solver. The results of the voltage current (VI) characteristics curve were compared with experimental results for validation [13, 21] and found satisfactory as shown in fig. 2. The average percentages of deviation from experimental values (considering active loss and ohmic loss zone) are 2.57% and 4.44%. The present model graph started to deviate from 0.5 V onwards significantly. The possible reason behind the deviation is the single-phase model which does not account for liquid water formation whereas that can be observed during experimentation. Hence modeling values are greater than the experimental values in the concentration loss zone.

Results and discussion

Independent effect of operating parameters

To compare the effect of different combinations of significant operating parameters, the independent effect study of operating parameters is done. The chosen operating parameters are anode inlet relative humidity, cathode inlet relative humidity, operating pressure, and nature of cathode gas. The results are shown in figs. 3-6 along with the given input conditions.

From fig. 3, it is evident that at 0.65 V, the higher inlet anode gas relative humidity curve performed 0.86% better than the lower inlet gas anode gas relative humidity in terms of power

Table 1. Boundary conditions

Boundary condition type	Parameters	Values
Velocity Inlet	Velocity inlet	2 m/s
	Mass fraction of H ₂	0.3
	Mass fraction of H ₂ O	0.7
	Velocity inlet	2 m/s
	Mass fraction of O ₂	0.2
	Mass fraction of H ₂ O	0.14
Pressure outlet	Anode outlet gas pressure	0 bar (gage)
	Anode inlet temperature	353 K
	Cathode outlet gas pressure	0 bar (gage)
	Cathode inlet temperature	353 K
Wall	Anode specified electric potential	0 V
	Cathode specified electric potential	1 to 0.4 V
	MEA temperature	353 K
	Faces: heat flux	0

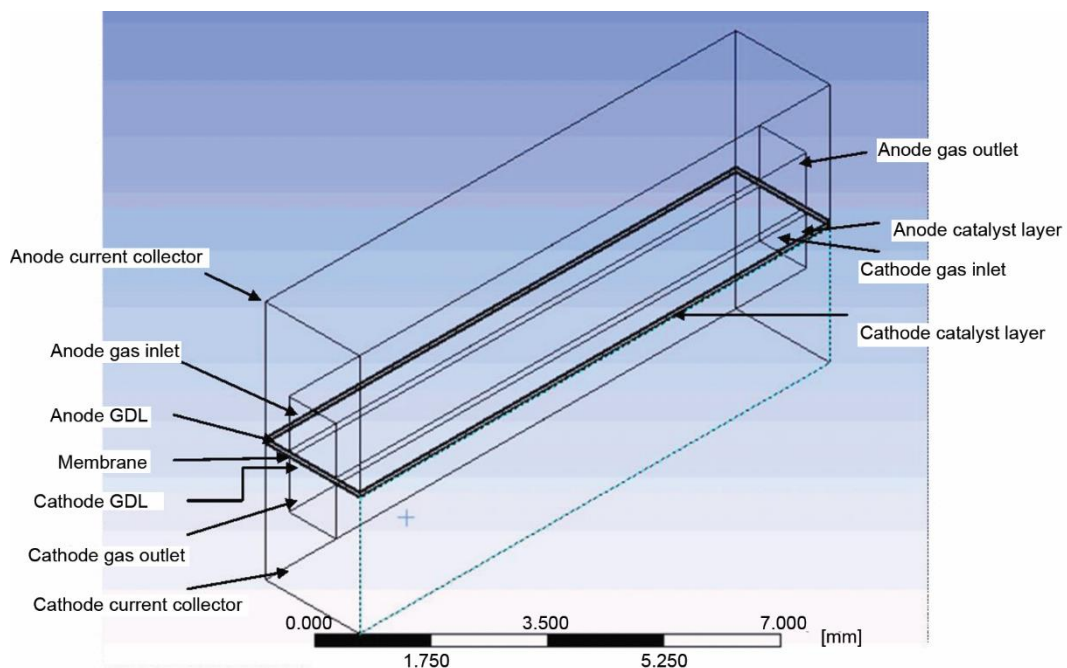


Figure 1. Geometry of the PEMFC model

density due to better reaction kinetics and proton conductivity. From fig. 4, it is clear that the higher inlet cathode gas relative humidity curve performed 5.93% better (at 0.65 V) than the lower inlet cathode gas relative humidity in terms of power density with similar possible reasons. From fig. 5, the higher operating pressure curve performed 29.39% better than the lower operating pressure in terms of power density at the same voltage due to better reaction kinetics with the aid of better diffusion of molecules through the membrane and higher exchange current density. It is concluded from fig. 6, that the oxygen curve performed 26.64% better than the air curve in terms of power density due to the high partial pressure of oxygen compared to air under similar conditions. The pattern of results is coincided with the literature [17].

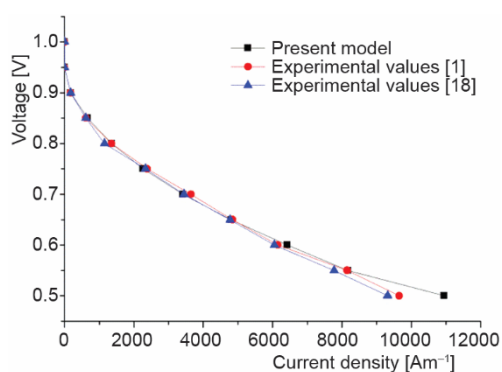


Figure 2. Validation of present model with experimental values

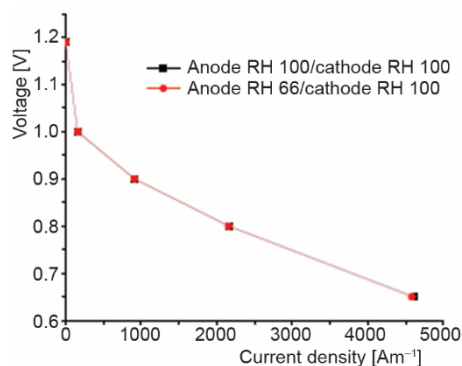


Figure 3. The VI curve for the different anode gas inlet relative humidity

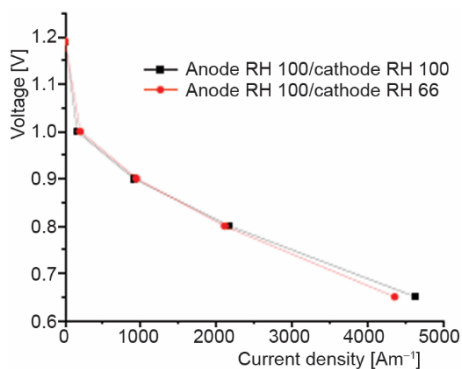


Figure 4. The VI curve for the different cathode gas inlet relative humidity

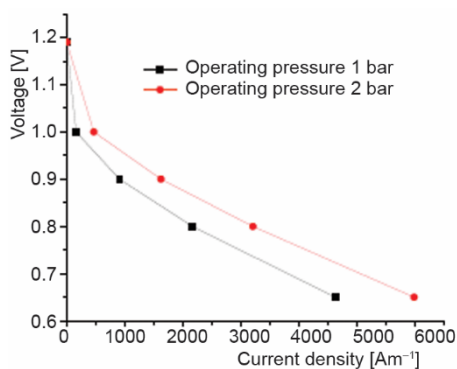


Figure 5. The VI curve for the different operating pressure

Combined effect of operating parameters

The chosen significant operating parameters are grouped in four different combinations namely Combination 1 (effect of the anode and cathode gas inlet RH), Combination 2 (anode and cathode inlet RH and operating pressure), Combination 3 (operating pressure and nature of cathode gas), and Combination 4 (anode and cathode inlet RH, operating pressure, and nature of cathode gas), and its effect on the performance of PEMFC is studied with the help of polarization VI curves.

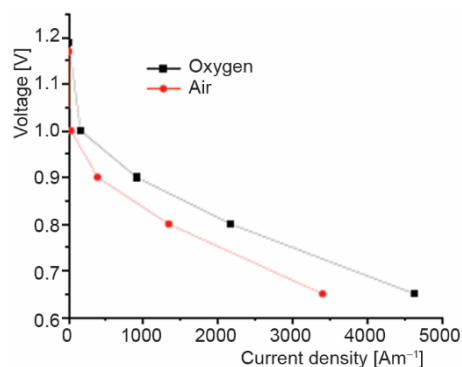


Figure 6. The VI curve for the different nature of cathode gas

the expected summation of the individual drop of 0.85% and 5.93%, respectively, when the anode and cathode gas RH varied independently to the same final value. This results in a surge of 1.34% reduced performance compared to simple summation. The combined reduction of RH leads to membrane dehydration at both anode and cathode sides, and *vice versa*. This paves the way for a reduction in both cathode and anode membrane conductivity, less reaction kinetics at both sides, and back diffusion of water molecules from the cathode side. Hence it is evident that the symmetric relative humidity reduction of both anode and cathode gas will be having a more significant performance drop compared to asymmetric relative humidity reduction and vice versa.

Combination 2 (C2)

Anode and cathode inlet relative humidity and operating pressure

Operating pressure, anode, and cathode gas inlet RH (1 bar, 66% and 66% to 2 bar 100% and 100%) were varied whereas all the other parameters like operating temperature, 353 K, nature of cathode gas, oxygen, inlet anode and cathode gas temperatures, 353 K and 343 K, were kept constant for both sets. The VI characteristics curve is shown in fig. 8.

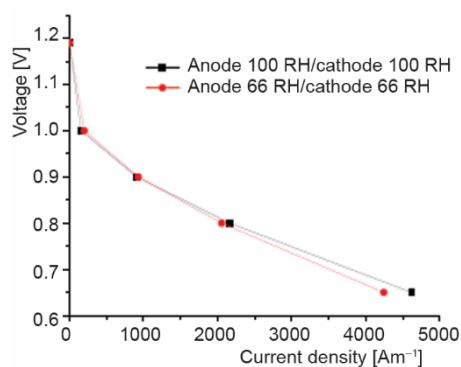


Figure 7. The VI curve for the different anode and cathode gas inlet RH

Combination 1 (C1)

Effect of anode and cathode gas inlet relative humidity

Both anode and cathode gas inlet RH (100% and 100% to 66% and 66%) were varied and all the other parameters like operating pressure, 1 bar, operating temperature, 353 K, nature of cathode gas, oxygen, inlet anode and cathode gas temperatures, 353 K and 343 K, were kept constant for both sets. The VI characteristics curve is shown in fig. 7.

At 0.65 V, the lower inlet anode and cathode gas RH curve performed 8.12% less than the higher inlet anode and cathode gas RH in terms of power density. This combined effect is lesser than

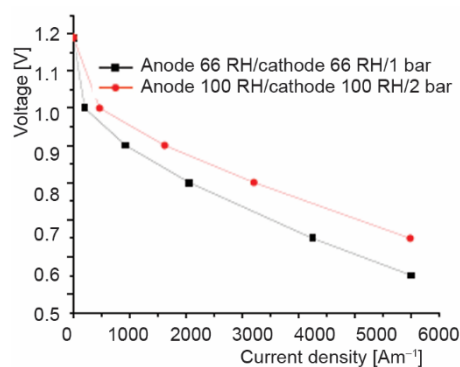


Figure 8. The VI curve for the different anode and cathode inlet RH and operating pressure

At 0.65 V, the higher operating pressure, inlet anode, and cathode gas RH curve performed 40.83% better than the lower operating pressure, inlet anode, and cathode gas RH in terms of power density. This combined effect is slightly less by 1.48% than the expected summation of the individual benefit of 32.02%, 2.38%, and 7.91%, respectively, when operating pressure, anode and cathode gas RH varied separately to the same final value. The possible reason for the slight reduction in the benefit at higher operating pressure, inlet anode, and cathode gas RH may be the diminished effect of high operating pressure in completely saturated gases compared to unsaturated reactant gases. Condensation of water vapor at a higher operating pressure of saturated vapor will be more compared to unsaturated reactant gases which may cause a slight reduction in the performance.

Combination 3(C3)

Operating pressure and nature of cathode gas

Operating pressure and nature of cathode gas (1 bar oxygen to 2 bar air) were varied whereas all the other parameters like the anode and cathode gas inlet RH, 100% both, operating temperature, 353 K, inlet anode and cathode gas temperatures, 353 K and 343 K, were kept constant for both sets. The VI characteristics curve is shown in fig. 9. At 0.65 V, air at the higher operating pressure curve performed 0.27% better than the lower operating pressure oxygen curve. As per the independent effect explanations, an increase in operating pressure should increase the performance and for the conversion of oxygen to air diminish the same. Here in the combined effect, the effect of operating pressure dominated compared to the change of nature of cathode gas to air. Hence the air curve performed slightly better than the oxygen curve. This combined effect is slightly less by 2.48% than the expected summation of the individual benefit of 29.39% and -26.64%, respectively, when operating pressure and nature of cathode gas varied separately without changing the mass-flow rate.

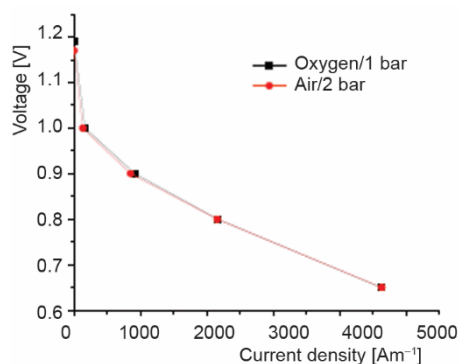


Figure 9. The VI curve for the different operating pressure and nature of cathode gas

The possible reason for a slight reduction in the benefit is the reduced benefit of air in a combined environment with higher operating pressure compared to the benefit of oxygen at a higher operating pressure despite the same mass-flow rate. The partial pressure of oxygen in the air will be lesser compared to pure oxygen. Hence higher operating pressure with air may give better results but with a certain shortage of complete benefit in the combined environment.

Combination 4 (C4)

Anode and cathode inlet relative humidity, operating pressure, and nature of cathode gas

Operating pressure, anode and cathode inlet RH, and nature of cathode gas (1 bar, 100%, 100% oxygen to 2 bar, 66%, 66% air) were varied whereas all the other parameters like operating temperature, 353 K, inlet anode and cathode gas temperatures, 353 K and 343 K, were kept constant for both sets. The VI characteristics curve is shown in fig. 10.

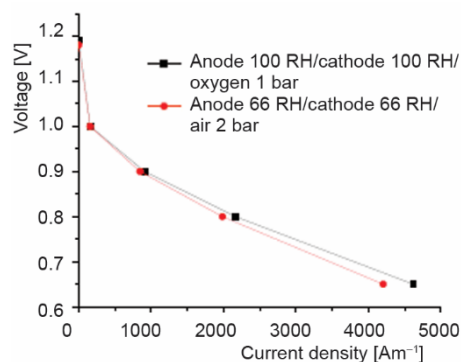


Figure 10. The VI curve for different anode and cathode inlet RH, operating pressure, and nature of cathode gas

be due to the combination of a reduction in both anode and cathode RH along with the nature of cathode gas as air which will dehydrate the membrane significantly than the independent effect.

Conclusion

A lot of researches has been concentrated on the effect of operating parameters on the performance of PEMFC but with the condition of keeping operating parameters other than analyzing parameters as constant. But in most of the practical applications, the variation of one operating parameter will lead to changes in other operating parameters and hence the effect of combined study will be more significant and relevant. The results of the independent effect of the operating parameters study are coherent with the literature. The combined operating parameters effect on the performance of the PEMFC study revealed that almost all combinations (C1: 1.34%, C2: 1.48%, C3: 2.48%, C4: 4.97%) affected the expected individual summation with significant percentage deviation. This is due to the dominance of one or more operating parameters in a combined environment than the independent effect study. Hence the positive combinations of operating parameters can be applied in practical applications which will give more benefit than the independent parameters variations and *vice versa*. The observed readings are limited to activation loss and ohmic loss zone due to single-phase modeling. The multiphase modeling and multiple combination studies are the future scopes that can further strengthen the present study.

Acknowledgment

The authors would like to thank the PSG Management for the motivation, technical support and computing facilities to complete the research.

Nomenclature

C_{H_2} – local concentration of hydrogen, [molm ⁻³]	k – electrical conductivity of bipolar plate [Sm ⁻¹]
$C_{H_2}^{ref}$ – reference concentration of hydrogen, [molm ⁻³]	M – molecular weight, [kgmol ⁻¹]
C_{O_2} – local concentration of oxygen, [molm ⁻³]	R_{an} – exchange current density of anode, [Am ⁻³]
$C_{O_2}^{ref}$ – reference concentration of oxygen, [molm ⁻³]	R_{cat} – exchange current density of cathode, [Am ⁻³]
F – Faraday's constant, [Cmol ⁻¹]	R_{ohm} – ohmic resistance, [Ω]
I – electrical current, [A]	S_i – mass sink term [kgs ⁻¹ m ⁻³]

At 0.65 V, higher operating pressure, lower RH, air curve performed 9.00% lesser than lower operating pressure, high RH, oxygen curve. Increased operating pressure induces a positive effect whereas the lower RH and nature of cathode gas promotes a negative effect in performance. Here the effect of RH and nature of cathode gas surpassed the benefit of operating pressure. This combined effect is even lesser by 4.97% than the expected summation of individual effect of -0.85%, -5.93%, 29.39%, and -26.64%, respectively, when anode and cathode RH, operating pressure, and nature of cathode gas varied separately without changing other parameters. The possible reason for higher surge than expected in the performance may

T – temperature, [K]
 u – x -direction velocity, [ms^{-1}]
 v – y -direction velocity, [ms^{-1}]
 w – z -direction velocity, [ms^{-1}]

Greek symbols

α_{an} – anode charge transport coefficient
 α_{cat} – cathode charge transport coefficient
 β – electrode diffusivity, [m^2]
 γ – concentration parameter
 ε – porosity
 η – surface overvoltage, [V]

μ – dynamic viscosity, [kgsm^{-2}]
 ρ – density, [kgm^{-3}]
 σ_{mem} – electrical conductivity of membrane, [Sm^{-1}]
 σ_{sol} – electrical conductivity of electrode, [Sm^{-1}]
 φ – phase potential, [V]

Subscripts

an – anode
cat – cathode
mem – membrane
ohm – ohmic
sol – solid

References

- [1] Hashemi, F., et al., CFD Simulation of PEM Fuel Cell Performance: Effect of Straight and Serpentine Flow Fields, *Mathematical and Computer Modelling*, 55 (2012), 3-4, pp. 1540-1557
- [2] Dutta, S., et al., Numerical Prediction of Mass-Exchange Between Cathode and Anode Channels in a PEM Fuel Cell, *International Journal of Heat and Mass Transfer*, 44 (2001), 11, pp. 2029-2042
- [3] Berning, T., et al., Three-Dimensional Computational Analysis of Transport Phenomena in a PEM Fuel Cell, *Journal of power sources*, 106 (2002), 1-2, pp. 284-294
- [4] Kumar, A., Reddy, R. G., Effect of Channel Dimensions and Shape in the Flow-Field Distributor on the Performance of Polymer Electrolyte Membrane Fuel Cells, *Journal of power sources*, 113 (2003), 1, pp. 11-18
- [5] Saco, S. A., et al., A Study on Scaled Up Proton Exchange Membrane Fuel Cell with Various Flow Channels For Optimizing Power Output by Effective Water Management Using Numerical Technique, *Energy* 113 (2016), Oct., pp. 558-573
- [6] Yan, W. M., et al., Numerical Study on Cell Performance and Local Transport Phenomena of PEM Fuel Cells with Novel Flow Field Designs, *Journal of Power Sources*, 161 (2006), 2, pp. 907-919
- [7] Sivertsen, B. R., Djilali, N., CFD-Based Modelling of Proton Exchange Membrane Fuel Cells, *Journal of Power Sources*, 141 (2005), 1, pp. 65-78
- [8] Jeon, D. H., et al., The Effect of Serpentine Flow-Field Designs on PEM Fuel Cell Performance, *International Journal of Hydrogen Energy*, 33 (2008), 3, pp. 1052-1066
- [9] Hashemi, F., et al., CFD Simulation of PEM Fuel Cell Performance: Effect of Straight and Serpentine Flow Fields, *Mathematical and Computer Modelling*, 55 (2012), 3-4, pp. 1540-1557
- [10] Jang, J. H., et al., Humidity of Reactant Fuel on the Cell Performance of PEM Fuel Cell with Baffle-Blocked Flow Field Designs, *Journal of power sources*, 159 (2006), 1, pp. 468-477
- [11] Robin, C., et al., Development and Experimental Validation of a PEM Fuel Cell 2D-Model to Study Heterogeneities Effects Along Large-Area Cell Surface, *International Journal of Hydrogen Energy*, 40 (2015), 32, pp. 10211-10230
- [12] Kang, S., Quasi-Three Dimensional Dynamic Modeling of a Proton Exchange Membrane Fuel Cell with Consideration of Two-Phase Water Transport Through a Gas Diffusion Layer, *Energy*, 90 (2015), Oct., pp. 1388-1400
- [13] Praveenkumar, S., et al., Influence of Pressure and Temperature on the Performance of Pem Fuel Cell with Taper Flow Channel Design, *International Journal of Applied Chemistry*, 11 (2015), 4, pp. 505-513
- [14] Kahveci, E. E., Taymaz, I., Experimental Investigation on Water and Heat Management in a PEM Fuel Cell Using Response Surface Methodology, *International journal of hydrogen energy*, 39 (2014), 20, pp. 10655-10663
- [15] Jang, J. H., et al., Numerical Study of Reactant Gas Transport Phenomena and Cell Performance of Proton Exchange Membrane Fuel Cells, *Journal of Power Sources*, 156 (2006), 2, pp. 244-252
- [16] Wang, L., et al., A Parametric Study of PEM Fuel Cell Performances, *International journal of hydrogen energy*, 28 (2003), 11, pp. 1263-1272
- [17] Ozen, D. N., et al., Effects of Operation Temperature and Reactant Gas Humidity Levels on Performance of PEM Fuel Cells, *Renewable and Sustainable Energy Reviews*, 59 (2016), June, pp. 1298-1306
- [18] Awan, A., et al., Simulation of Proton Exchange Membrane Fuel Cell by using ANSYS Fluent, *Materials Science and Engineering*, 414 (2018), ID 012045

- [19] Xia, Z., *et al.*, Effect of Operating Conditions on Performance of Proton Exchange Membrane Fuel Cell with Anode Recirculation, *Energy Procedia*, 158 (2019), Feb., pp. 1829-1834
- [20] Xing, L., *et al.*, A Two-Phase Flow and Non-Isothermal Agglomerate Model for a Proton Exchange Membrane (PEM) Fuel Cell, *Energy*, 73 (2014), Aug., pp. 618-634
- [21] Babu, A. R., *et al.*, Effect of Design and Operating Parameters on the Performance of Planar and Ducted Cathode Structures of an Air-Breathing PEM Fuel Cell, *Arabian Journal for Science and Engineering*, 41 (2016), 9, pp. 3415-3423
- [22] Malekbalaa, *et al.*, Modeling and Control of a PEM Fuel Cell with the Air Compressor According to Requested Electrical Current, *Thermal Science*, 19 (2014), 6, pp. 2065-2078
- [23] Babu, A. R., *et al.*, Parametric Study of the Proton Exchange Membrane Fuel Cell for Investigation of Enhanced Performance Used in Fuel Cell Vehicles, *Alexandria Engineering Journal*, 57 (2018), 4, pp. 3953-3958
- [24] Lim, B. H., *et al.*, Three-Dimensional Study of Stack on the Performance of the Proton Exchange Membrane Fuel Cell, *Energy*, 169 (2019), Feb., pp. 338-343
- [25] Shah, A. A., *et al.*, Recent Trends and Developments in Polymer Electrolyte Membrane Fuel Cell Modeling, *ElectrochimicaActa*, 56 (2011), 11, pp. 3731-3757
- [26] Bose, S., *et al.*, Polymer Membranes for High Temperature Proton Exchange Membrane Fuel Cell: Recent Advances and Challenges, *Progress in Polymer Science*, 36 (2011), 6, pp. 813-43
- [27] Yuan, X. Z., *et al.*, A Review of Polymer Electrolyte Membrane Fuel Cell Durability Test Protocols, *Journal of Power Sources*, 196 (2011), 22, pp. 9107-9116
- [28] Kandlikar, S. G., Lu, Z., Thermal Management Issues in a PEMFC Stack—A Brief Review of Current Status, *Applied Thermal Engineering*, 29 (2009), 7, pp. 1276-80
- [29] Erdinc, O., Uzunoglu, M., Recent Trends in PEM Fuel Cell-Powered Hybrid Systems: Investigation of Application Areas, Design Architectures and Energy Management Approaches, *Renewable and Sustainable Energy Reviews*, 14 (2010), 9, pp. 2874-2884
- [30] Chandan, A., *et al.*, High Temperature (HT) Polymer Electrolyte Membrane Fuel Cells (PEMFC) – A Review, *Journal of Power Sources*, 231 (2013), June, pp. 264-278
- [31] Yonoff, R. E., *et al.*, Research Trends in Proton Exchange Membrane Fuel Cells During 2008–2018: A Bibliometric Analysis, *Heliyon*, 5 (2019), 5, pp. e017-24